Generalized Frequency Domain Modeling and Analysis For A Flexible Rotating Spacecraft

Tarek A. Elgohary[*] and James D. Turner [†]

Texas A&M University, College Station, Texas, 77843-3141, US.

A flexible rotating spacecraft is modeled as a three body hybrid system consisting of a rigid hub a flexible appendage following the Euler-Bernoulli beam assumptions and a tip mass and inertia. Hamilton's extended principle is used to derive the equations of motion and the boundary conditions of the system. This work compares the frequency domain accuracy provided by series approximation methods versus analytical models. Applying the Laplace transform to the integro-partial derivation equations of motion model, leads to a generalized state space model for the frequency domain representation of the system. Both approximate and exact transfer function models are developed and compared. Eigen decomposition is used to solve the flexible appendage sub-problem and then to find the solution for the full system of equations. The analytic frequency domain model is manipulated by introducing a spatial domain state space, where a standard convolution integral representation is used to invoke the boundary conditions that act at the tip mass for the free end of the beam. Closed-form solutions are obtained for the convolution integral forcing terms. The closed form solution is used to generate transfer functions for both the rigid and the flexible modes of the system in terms of the input torque. A numerical example is presented to compare the frequency response of the closed form solution transfer function to the numerical assumed modes solution. The difference resulting from in the natural frequencies resulting from the series truncation is highlighted and discussed. The closed form solution proves to be more accurate with no truncation errors and is suitable for control design iterations.

Nomenclature

E	Appendage Young's modulus
I	Moment of inertia of appendage cross section about centroidal axis
I_{hub}	Rigid hub moment of intertia
I_{tip}	Tip mass rotary inertia
L	Appendage length
ρ	Appendage mass per unit length
m	Tip mass
r	Hub radius
$()'$	$\frac{d}{dx}$
$\dot{()}$	$\frac{d}{dt}$
θ	Hub rotation
y	Appendage deformation
V_L	Left eignevectors
V_R	Right eigenvectors

*Graduate Research Assistant, Texas A&M University, Aerospace Engineering Department, 701 H.R. Bright Building, 3141 TAMU, College Station, Texas 77843-3141, AIAA Student Member.

†Research Professor, Texas A&M University, Aerospace Engineering Department, 701 H.R. Bright Building, 3141 TAMU, College Station, Texas 77843-3141.

I. Introduction

Modeling a rotating flexible spacecraft as a coupled rigid-flex hybrid system is a widely used modeling practice for the dynamics and controls of such systems. Both Lagrangian and Eulerian approaches have been introduced in several works to derive the governing equations for hybrid systems. A comparison between the two approaches is introduced in[1] where both methods produced the same results but the Eulerian approach proved to provide a better insight on physics of the problem. In general, the resulting equations are coupled integral partial differential equations developed in several works,.[2-5] Solutions techniques presented in these works are mainly numerical with finite elements methods and/or assumed modes techniques. Numerical solutions in general are approximate and the accuracy is a function of the number of elements/modes chosen which can impose a high computational cost as the need arises for more accurate results.

As a control problem, single axis rotating flexible spacecraft is addressed extensively utilizing several controls and modeling schemes. The optimal control problem of a rotating hub with symmetric four flexible appendages is presented as a numerical example in.[6] The linearized system is constructed using the assumed modes approach by defining an admissible function that is both differentiable and satisfies geometric boundary conditions. The effectiveness of the minimization of the presented cost function is found to rely on the number of modes retained in the series of the chosen admissible function and the small deflection assumptions. The same problem is also addressed in[4] where both finite elements techniques and the assumed approach are used to construct the linearized problem. The natural frequencies of the system has been calculated by solving the generalized eigenvalue problem and the various methods are compared in terms of accuracy and the number of terms required to achieve it. Several other flexible structures examples including the single axis rotating hub with four symmetric identical flexible appendages are presented in.[7] The optimal control problem is again addressed for various control schemes and penalty functions including free final time, free final angle and control rate penalty methods. Large angle maneuvers for a flexible spacecraft is addressed in[8] where a similar hub-four flexible appendages model is analyzed and the optimal control problem for it is formulated addressing kinematic nonlinearities and the two-point boundary value problem. In[9] large angle maneuvers for the same model are considered. The optimal control problem with a distributed control scheme is addressed and an iterative continuation technique is utilized to address the kinematics nonlinearities. In a more recent work[10] addressed the adaptive control problem for a similar rigid hub flexible appendage model. The proposed control scheme is independent of the truncation generated from the flexible modes admissible function because no series approximations are introduced. The system modeling parameters are explicitly handled in the governing integro-partial differential equation of motion model. Several other works[11-16] address similar problems with emphasis on optimality,[11-13] and/or robustness,.[15,16] In the controls and robotics community the same models are used in flexible robotic arm manipulators dynamics and controls.[17] provides a comprehensive review of the literature in this area focusing on works in the various robotics communities. The major contribution of this work in the development of a exact transfer function model for a rotating flexible beam.

In[18] an analytical transfer function for a rotating flexible spacecraft modeled as a rigid hub attached to a free end flexible beam is introduced. The transfer function is used to analyze the frequency response of the hybrid system. Numerical results are compared and verified against the assumed modes solution where the truncation in the series solution is highlighted. In this paper, a more complicated model is proposed by adding a tip mass with inertia at the end of the flexible beam which leads to more complicated boundary conditions that must be enforced in the frequency domain. A generalized state state space model is constructed and solved by means of eigen decomposition. A transformation to a more tractable complex representation is used to develop frequency domain based closed form solution. The transfer function for the flexible mode is then derived and the frequency response versus the assumed modes solution is compared. The development of the closed form frequency response of the proposed model has several benefits in understanding the system behavior and its exact natural frequencies. Also it can be utilized in developing accurate control schemes that benefits from the existence of the exact solution.

II. The Model

The flexible spacecraft is modeled as a rotating rigid hub attached to a cantilevered flexible appendage with a concentrated tip mass/inertia at its end as shown in figure 1. The hub rotates about its z-axis and the appendage is allowed to have transverse motion about its y-axis. The appendage follows the standard

American Institute of Aeronautics and Astronautics

Euler-Bernoulli assumptions with negligible shear deformation and negligible distributed rotary inertia. The system equations of motion and boundary conditions are derived using the extended Hamilton's principle.[19] The equations are linearized by dropping the coupling term $y\dot{\theta}$. The inertial position of a point on the flexible appendage is given by,

$$\mathbf{p} = (x + r)\,\hat{\mathbf{b_1}} + y\hat{\mathbf{b_2}} \tag{1}$$

The velocity can then be expressed as,

$$\mathbf{v} = \dot{y}\hat{\mathbf{b_2}} + \dot{\theta}\hat{\mathbf{b_3}} \times \left[(x + r)\,\hat{\mathbf{b_1}} + y\hat{\mathbf{b_2}}\right] \tag{2}$$

Neglecting the $y\dot{\theta}$ term in the velocity, the kinetic energy is then expressed as,[4]

$$T = T_{\text{hub}} + T_{\text{appendage}} + T_{\text{tip}}$$

$$T = \frac{1}{2}I_{\text{hub}}\dot{\theta}^2 + \frac{1}{2}\int_0^L \rho\left(\dot{y} + (x + r)\dot{\theta}\right)^2 dx + \frac{1}{2}m\left((r + L)\dot{\theta} + \dot{y}(L)\right)^2 + \frac{1}{2}I_{\text{tip}}\left(\dot{\theta} + \dot{y}'(L)\right)^2 \tag{3}$$

The potential energy for the flexible appendage is given by

$$V = \frac{1}{2}\int_0^L EI\,(y'')^2\,dx \tag{4}$$

The Lagrangian is given by,

$$\mathcal{L} = T - V$$

$$\mathcal{L} = \frac{1}{2}I_{\text{hub}}\dot{\theta}^2 + \frac{1}{2}\int_0^L \left\{\rho\left(\dot{y} + (x + r)\dot{\theta}\right)^2 - EI\,(y'')^2\right\} dx + \frac{1}{2}m\left((r + L)\dot{\theta} + \dot{y}(L)\right)^2 + \frac{1}{2}I_{\text{tip}}\left(\dot{\theta} + \dot{y}'(L)\right)^2 \tag{5}$$

Applying Hamilton's extended principle, the system governing equations of motion are,

$$I_{\text{hub}}\ddot{\theta} + \int_0^L \rho(x + r)\left(\ddot{y} + (x + r)\ddot{\theta}\right) dx + m(L + r)\left((L + r)\ddot{\theta} + \ddot{y}(L)\right) + I_{\text{tip}}\left(\ddot{\theta} + \ddot{y}'(L)\right) = u \tag{6}$$

$$\rho\left(\ddot{y} + (x + r)\ddot{\theta}\right) + EIy^{IV} = 0$$

Boundary conditions are also extracted from Hamilton's extended principle as,

$$\text{at } x = 0 : y = 0, \quad y' = 0$$

$$\text{at } x = L : EI\frac{\partial^3 y}{\partial x^3}\bigg|_L = m\left((L + r)\ddot{\theta} + \ddot{y}(L)\right), \quad EI\frac{\partial^2 y}{\partial x^2}\bigg|_L = -I_{\text{tip}}\left(\ddot{\theta} + \ddot{y}'(L)\right) \tag{7}$$

III.   Generalized State Space (GSS)

Following the same approach presented in,[18] a Generalized State Space system (GSS) is derived to express the hybrid system in the frequency domain. First the Laplace transform of the equations of motion, Eq. (6), is expressed as

$$\mu^2 J\bar{\theta} + \mu^2 \rho \int_0^L (r + x)\bar{y}dx + \mu^2 m(r + L)\bar{y}(L) + \mu^2 I_{\text{tip}}\bar{y}'(L) = \bar{u}$$

$$\mu^2 \rho\left(\bar{y} + (x + r)\bar{\theta}\right) + EI\bar{y}^{IV} = 0 \tag{8}$$

$$\text{where,} \quad J \equiv I_{\text{hub}} + m(r + L)^2 + I_{\text{tip}} + \int_0^L \rho(r + x)^2 dx$$

Integration by parts is then utilized to decouple the deformation parameter y from the spatial variable x such that,

$$\int_0^L (r + x)\bar{y}\,dx = (r + x)\int_0^L \bar{y}\,dx - \iint \bar{y}\,dx\,dx' \tag{9}$$

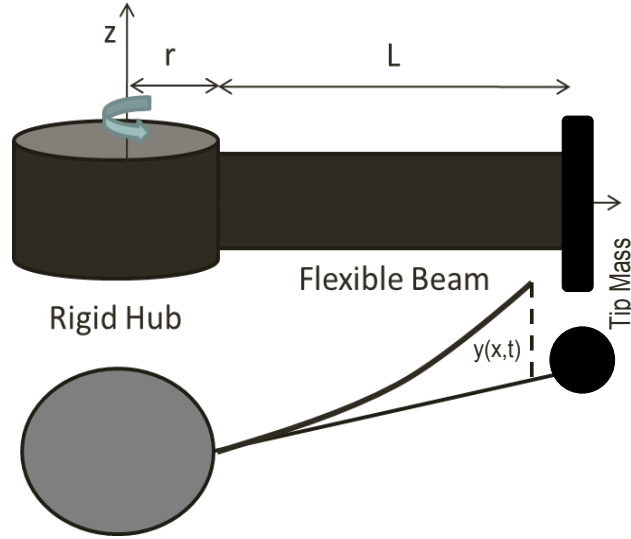American Institute of Aeronautics and Astronautics

Figure 1. Flexible robotic arm manipulator with payload

Plugging Eq. (9) into Eq. (8) yeilds the generalized integral equation,

$$\mu^2 J\bar{\theta} + \mu^2 \rho \left((x+r) \int_0^L \bar{y}\,\mathrm{d}x - \iint \bar{y}\,\mathrm{d}x\,\mathrm{d}x' \right) + \mu^2 m(r+L)\bar{y}(L) + \mu^2 I_{\text{tip}}\bar{y}'(L) = \bar{u}$$

(10)

$$\frac{\mu^2 \rho}{EI}\left(\bar{y} + (x+r)\bar{\theta}\right) + \bar{y}^{IV} = 0$$

Similar to the equations of motion the boundary conditions are expressed in the Laplace/frequency domain as,

$$\text{at } x = 0 : \bar{y} = 0, \quad \bar{y}' = 0$$

$$\text{at } x = L : \bar{y}''' = \frac{\mu^2 m}{EI}\left[(r+L)\bar{\theta} + \bar{y}(L)\right], \quad \bar{y}'' = -\frac{\mu^2 I_{\text{tip}}}{EI}\left[\bar{y}'(L) + \bar{\theta}\right]$$

(11)

Eq. (10) leads to the definition of the state space system,

$$
\begin{array}{ll}
z_1 = \iint \bar{y}\,\mathrm{d}x\,\mathrm{d}x' & z_1' = z_2 \\
z_2 = \int \bar{y}\,\mathrm{d}x & z_2' = z_3 \\
z_3 = \bar{y} & z_3' = z_4 \\
z_4 = \bar{y}' & z_4' = z_5 \\
z_5 = \bar{y}'' & z_5' = z_6 \\
z_6 = \bar{y}''' & z_6' = -\beta\left(z_3 + (r+x)\bar{\theta}\right)
\end{array}
\qquad \text{where, } \beta \equiv \frac{\mu^2 \rho}{EI}
$$

(12)

with the associated boundary conditions,

$$\text{at } x = 0 : \{Z\} = \begin{bmatrix} 0 & 0 & 0 & 0 & z_5 & z_6 \end{bmatrix}^{\mathrm{T}}$$

$$\text{at } x = L : z_5(L) = -\alpha\left[z_4(L) + \bar{\theta}\right], \quad z_6(L) = \gamma\left[z_3(L) + (r+L)\bar{\theta}\right]$$

(13)

$$\text{where, } \alpha \equiv \frac{\mu^2 I_{\text{tip}}}{EI} \quad \text{and} \quad \gamma \equiv \frac{\mu^2 m}{EI}$$

American Institute of Aeronautics and Astronautics

The GSS is represented in the forced linear differential form $\{Z'\} = [A]\{Z\} + \{b\}$ as,

$$\{Z'\} = \begin{bmatrix} 0 & 1 & 0 & 0 & 0 & 0 \\ 0 & 0 & 1 & 0 & 0 & 0 \\ 0 & 0 & 0 & 1 & 0 & 0 \\ 0 & 0 & 0 & 0 & 1 & 0 \\ 0 & 0 & 0 & 0 & 0 & 1 \\ 0 & 0 & -\beta & 0 & 0 & 0 \end{bmatrix} \begin{Bmatrix} z_1 \\ z_2 \\ z_3 \\ z_4 \\ z_5 \\ z_6 \end{Bmatrix} + \begin{Bmatrix} 0 \\ 0 \\ 0 \\ 0 \\ 0 \\ -\beta(x+r)\bar{\theta} \end{Bmatrix} \tag{14}$$

which along with the boundary conditions in Eq. (13) defines a 6×6 linear system of equations that describes the frequency response of the hybrid dynamical system.

III.A. Beam sub-problem solution

The full solution of the 6×6 GSS systems starts by solving the 4×4 sub-matrix which defines the unforced beam sub-problem. The beam sub-problem can be expressed as a 4×4 system of equations as,

$$\{p'\} = [Q]\{p\}$$

where,

$$[Q] = \begin{bmatrix} 0 & 1 & 0 & 0 \\ 0 & 0 & 1 & 0 \\ 0 & 0 & 0 & 1 \\ -\beta & 0 & 0 & 0 \end{bmatrix} \tag{15}$$

Equation (15) is solved by obtaining the matrix exponential,,[20] of $[Q]$ or $\exp[Qx]$ by using eigen decomposition. First, the eigenvalues of $[Q]$ are obtained

$$\Lambda = \beta^{1/4}\mathrm{Diag}\begin{bmatrix} -\dfrac{1}{\sqrt{i}} & -\sqrt{i} & \dfrac{1}{\sqrt{i}} & \sqrt{i} \end{bmatrix} \tag{16}$$

the right and left eigenvectors are then utilized to diagonalize $[Q]$ and obtain the matrix exponential solution as,

$$\exp[Qx] = V_R \exp[Dx]V_L^{\mathrm{T}}$$

$$\exp[Dx] = \begin{bmatrix} e^{-\frac{\beta^{1/4}}{\sqrt{i}}x} & 0 & 0 & 0 \\ 0 & e^{-\beta^{1/4}\sqrt{i}x} & 0 & 0 \\ 0 & 0 & e^{\frac{\beta^{1/4}}{\sqrt{i}}x} & 0 \\ 0 & 0 & 0 & e^{-\beta^{1/4}\sqrt{i}x} \end{bmatrix} \tag{17}$$

Equation (17) yields the matrix exponential solution in the form,

$$\exp[Qx] = \begin{bmatrix} f & -f'''/\beta & -f''/\beta & -f'/\beta \\ f' & f & -f'''/\beta & -f''/\beta \\ f'' & f' & f & -f'''/\beta \\ f''' & f'' & f' & f \end{bmatrix} \tag{18}$$

where the function representing the diagonal element in Eq. (18) is given by,

$$f(x) = \cos\left(\frac{\beta^{1/4}x}{\sqrt{2}}\right)\cosh\left(\frac{\beta^{1/4}x}{\sqrt{2}}\right) \tag{19}$$

American Institute of Aeronautics and Astronautics

III.B. Full GSS solution

The 6×6 GSS solution is then extracted from the beam sub-problem matrix exponential solution, Eq. (18), with a similar structure given by,

$$\exp[Ax] = \begin{bmatrix} 1 & x & -f''/\beta & -f'/\beta & (1-f)/\beta & (\beta x + f''')/\beta^2 \\ 0 & 1 & -f'''/\beta & -f''/\beta & -f'/\beta & (1-f)/\beta \\ 0 & 0 & f & -f'''/\beta & -f''/\beta & -f'/\beta \\ 0 & 0 & f' & f & -f'''/\beta & -f''/\beta \\ 0 & 0 & f'' & f' & f & -f'''/\beta \\ 0 & 0 & f''' & f'' & f' & f \end{bmatrix} \tag{20}$$

The full solution for the system is known to have the general form,,[20]

$$\{Z(x)\} = \underbrace{\exp[Ax]\{Z(0)\}}_{Z_H} + \underbrace{\int_0^x \exp\left[A(x-\tau)\right]\{b(\tau)\}\,\mathrm{d}\tau}_{Z_F} \tag{21}$$

The homogeneous solution Z_H is then given by,

$$\{Z_H\} = \left\{ \begin{array}{c} (1-f)z_5/\beta - (\beta x + f''')z_6/\beta^2 \\ -f'z_5/\beta + (1-f)z_6/\beta \\ -f''z_5/\beta - f'z_6/\beta \\ -f'''z_5/\beta - f''z_6/\beta \\ fz_5 - f'''z_6/\beta \\ f'z_5 + fz_6 \end{array} \right\} \tag{22}$$

The convolution integral in Eq. (21) is then evaluated to obtain the forced part of the GSS solution as,

$$\{Z_F\} = \int_0^x \exp\left[A(x-\tau)\right]\{b(\tau)\}\,\mathrm{d}\tau = -\beta\bar{\theta}\int_0^x (r+\tau) \left\{ \begin{array}{c} (\beta(x-\tau) + f'''(x-\tau))/\beta^2 \\ (1 - f(x-\tau))/\beta \\ -f'(x-\tau)/\beta \\ -f''(x-\tau)/\beta \\ -f'''(x-\tau)/\beta \\ f(x-\tau) \end{array} \right\} \,\mathrm{d}\tau \tag{23}$$

In order to fully present the solution in a tractable form, it is observed that the function f representing the various elements of the solution is the real part of the complex function

$$f = Re\{\cos(\sigma x)\}, \quad \text{where,}\ \sigma \equiv \sqrt{i\sqrt{\beta}} \tag{24}$$

Using Eq. (24) to represent f makes the homogeneous solution in Eq. (22) appear as,

$$\{Z_H\} = \left\{ \begin{array}{c} (1-\cos(\sigma x))z_5/\beta + (\beta x + \sigma^3\sin(\sigma x))z_6/\beta^2 \\ \sigma\sin(\sigma x)z_5/\beta + (1-\cos(\sigma x))z_6/\beta \\ \sigma^2\cos(\sigma x)z_5/\beta + \sigma\sin(\sigma x)z_6/\beta \\ -\sigma^3\sin(\sigma x)z_5/\beta + \sigma^2\cos(\sigma x)z_6/\beta \\ \cos(\sigma x)z_5 - \sigma^3\sin(\sigma x)z_6/\beta \\ -\sigma\sin(\sigma x)z_5 + \cos(\sigma x)z_6 \end{array} \right\} \tag{25}$$

The elements of convolution integral presneted in Eq. (23) can then be evluated as follows:

$$\begin{aligned} I_1(x) &= \tfrac{1}{6\beta}\left(-3\beta rx^2 - \beta x^3 + 6\sigma^2 r\cos(\sigma x) + 6\sigma\sin(\sigma x) - 6\sigma^2 r - 6\sigma^2 x\right)\bar{\theta} \\ I_2(x) &= \tfrac{1}{2\sigma^2}\left(-2\sigma^2 rx - \sigma^2 x^2 + 2\sigma r\sin(\sigma x) - 2\cos(\sigma x) + 2\right)\bar{\theta} \\ I_3(x) &= \tfrac{1}{\sigma}\left(\sigma r\cos(\sigma x) + \sin(\sigma x) - \sigma r - \sigma x\right)\bar{\theta} \\ I_4(x) &= \left(-\sigma r\sin(\sigma x) + \cos(\sigma x) - 1\right)\bar{\theta} \\ I_5(x) &= -\sigma\left(\sigma r\cos(\sigma x) + \sin(\sigma x) - \sigma r - \sigma x\right)\bar{\theta} \\ I_6(x) &= -\tfrac{1}{\sigma^2}\left(\beta\left(\sigma r\sin(\sigma x) - \cos(\sigma x) + 1\right)\right)\bar{\theta} \end{aligned} \tag{26}$$

American Institute of Aeronautics and Astronautics

Equations (25) and (26) are combined to produce the full GSS solution as a function of z_5 and z_6. $\bar{\theta}$ is taken out from the expressions of the convolution integrals presented in Eq. (26) to simplify the representation of the full solution.

$$\{Z(x)\} = \left\{ \begin{array}{c} (1 - \cos(\sigma x))z_5/\beta + (\beta x + \sigma^3 \sin(\sigma x))z_6/\beta^2 + I_1(x)\bar{\theta} \\ \sigma \sin(\sigma x)z_5/\beta + (1 - \cos(\sigma x))z_6/\beta + I_2(x)\bar{\theta} \\ \sigma^2 \cos(\sigma x)z_5/\beta + \sigma \sin(\sigma x)z_6/\beta + I_3(x)\bar{\theta} \\ -\sigma^3 \sin(\sigma x)z_5/\beta + \sigma^2 \cos(\sigma x)z_6/\beta + I_4(x)\bar{\theta} \\ \cos(\sigma x)z_5 - \sigma^3 \sin(\sigma x)z_6/\beta + I_5(x)\bar{\theta} \\ -\sigma \sin(\sigma x)z_5 + \cos(\sigma x)z_6 + I_6(x)\bar{\theta} \end{array} \right\} \tag{27}$$

To complete the closed form solution an expression for z_5 and z_6 in terms of the given system parameters is required. First, boundary conditions at the tip mass in Eq. (13) are imposed to express z_5 and z_6 as functions of $z_3(L)$ and $z_4(L)$ such that,

$$\left\{ \begin{array}{c} -\alpha \left(z_4(L) + \bar{\theta}\right) \\ \gamma \left(z_3(L) + (r+L)\bar{\theta}\right) \end{array} \right\} = \left[\begin{array}{cc} \cos(\sigma L) & -\sigma^3 \sin(\sigma L)/\beta \\ -\sigma \sin(\sigma L) & \cos(\sigma L) \end{array} \right] \left\{ \begin{array}{c} z_5 \\ z_6 \end{array} \right\} + \left\{ \begin{array}{c} I_5(L) \\ I_6(L) \end{array} \right\} \bar{\theta}$$

$$\left\{ \begin{array}{c} z_5 \\ z_6 \end{array} \right\} = \frac{1}{-\beta \cos(\sigma L)^2 + \sigma^4 \sin(\sigma L)^2} \tag{28}$$

$$\left\{ \begin{array}{c} (\beta(\alpha + I_5) \cos(\sigma L) - \sigma^3 \sin(\sigma L)(\gamma(r+L) - I_6))\bar{\theta} - \sigma^3\gamma \sin(\sigma x)z_3(L) + \alpha\beta \cos(\sigma x)z_4(L) \\ (\beta(\alpha + I_5) \sin(\sigma L) - \beta \cos(\sigma L)(\gamma(r+L) - I_6))\bar{\theta} - \beta\gamma \cos(\sigma x)z_3(L) + \alpha\beta\sigma \sin(\sigma x)z_4(L) \end{array} \right\}$$

The final step is to solve for $z_3(L)$ and $z_4(L)$ in terms of the given system parameters. This is done by substituting Eq. (28) in Eq. (27) and evaluating z_3 and z_4 at the tip of the beam. This results in a system of equations in $z_3(L)$ and $z_4(L)$ that can be solved as follows,

$$\left\{ \begin{array}{c} z_3(L) \\ z_4(L) \end{array} \right\} = \frac{1}{\beta} \left[\begin{array}{cc} \sigma^2 \cos(\sigma L) & \sigma \sin(\sigma L) \\ -\sigma^3 \sin(\sigma L) & \sigma^2 \cos(\sigma L) \end{array} \right] \left\{ \begin{array}{c} z_5 \\ z_6 \end{array} \right\} + \left\{ \begin{array}{c} I_3(L) \\ I_4(L) \end{array} \right\} \bar{\theta}$$

$$\left\{ \begin{array}{c} z_3(L) \\ z_4(L) \end{array} \right\} = \frac{\bar{\theta}}{-\sigma^5\gamma \sin(2\sigma L) + (2\alpha\gamma + \beta \cos(2\sigma L) - \beta)\sigma^4 - \sigma\beta\gamma \sin(2\sigma L) + \beta^2 (\cos(2\sigma L) + 1)}$$

$$\left\{ \begin{array}{c} \begin{array}{l} (r\gamma + \gamma L - I_6)\,\sigma^5 \sin(2\sigma L) + (\beta(\cos(2\sigma L) - 1)\,I_3 + 2\alpha(-\gamma L + I_6 - \gamma r))\,\sigma^4 \\ -2\beta(\alpha I_4 + \alpha + I_5)\,\sigma^2 + \beta(\gamma r + \gamma L - I_6)\,\sigma \sin(2\sigma L) + \beta^2 (\cos(2\sigma L) + 1)\,I_3 \end{array} \\ \\ \begin{array}{l} (\gamma(-I_3 - L - r) + I_6 + (\gamma r - I_6 + \gamma I_3 + \gamma L)\cos(2\sigma L))\,\sigma^6 - \gamma I_4\sigma^5 \sin(2\sigma L) \\ + (-2\gamma(\alpha + I_5) + \beta I_4 (\cos(2\sigma L) - 1))\,\sigma^4 \\ + (\beta\gamma(r + L + I_3) + \beta(I_6 + \gamma I_3 + \gamma L + \gamma r)\cos(2\sigma L) - \beta I_6)\,\sigma^2 \\ -I_4\beta\gamma\sigma \sin(2\sigma L) + \beta^2 (\cos(2\sigma L) + 1)\,I_4 \end{array} \end{array} \right\} \tag{29}$$

The solution of $z_3(L)$ and $z_4(L)$ in Eq. (29) concludes the full solution for Eq. (27). It must be highlighted that in order to maintain the validity of the solution and meet the physical boundary conditions at both ends of the flexible appendage, only the real part of the solution in Eq. (28) should be extracted to carry out the rest of the derivation presented in Eq. (29). The real part of the result is then plugged back in the full solution in Eq. (27) to represent the full GSS solution in terms of the given system parameters and the value of the frequency represented in the μ term appearing both explicitly and implicitly as part of α, β, γ and by definition σ. A numerical example is presented next to verify the validity of the GSS solution versus numerical integration and to verify that the boundary conditions at both ends of the flexible appendage are satisfied.

III.C.   Analytical solution vs. numerical integration

The closed form solution presented in the previous section is compared against numerical integration of system of equations in Eq. (14). Values from[4] are used for the various system parameters as shown in

Table 1. System Parameters Values

Parameter	Value	
I_{hub}	8	slug-ft^2
ρ	0.0271875	slug/ft
E	0.1584×10^{10}	lb/ft^2
L	4	ft
r	1	ft
I	0.47095×10^{-7}	ft^4
m	0.1569	slug
I_{tip}	0.0018	slug-ft^2

table 1, Arbitrary values of $\mu^2 = 4$ and $\bar{\theta} = 0.1$ are chosen in order to obtain values for α, β, γ and σ. Maple built in numerical integrator, $RK45$, is utilized and the results are plotted along with the analytical solution for the range of values of $x = 0 \cdots 4$ ft along the beam length. Figure 2 shows the response for z_3 vs. x using both the analytical and the numerical methods. Figure 3 shows the error between the two methods in z_3 along the length of the beam. Similar results of identical agreement can be obtained for the various variables
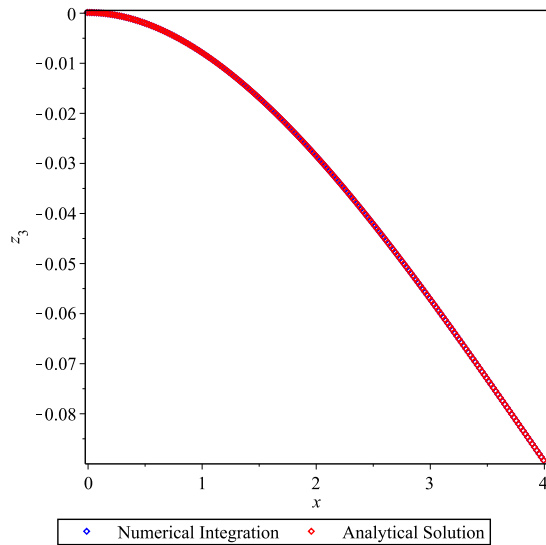
Figure 2. $z_3(x)$, numerical vs. analytical
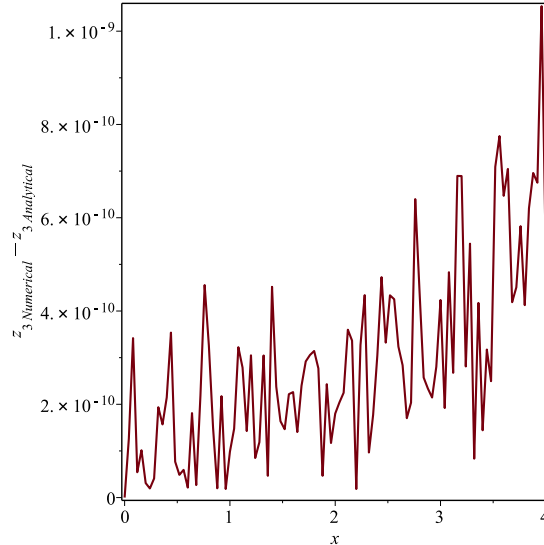
Figure 3. Error in $z_3(x)$ along appendage length

of the GSS model. Here, we are interested in z_3 which represents the flexible appendage frequency response $\bar{y}$ that will be the subject of further analysis of the input/output transfer function of the appendage.

IV. Flexible Appendage Frequency Response

The analytical solution for the GSS is used to generate the frequency response of the flexible appendage. The analytical solution is used to generate input/output transfer functions for both the rigid hub rotation and the flexible beam deformation. For verification the transfer function results is compared against the well known assumed modes method[4] to verify the appendage natural frequencies.

American Institute of Aeronautics and Astronautics

IV.A. GSS transfer function

From Eq. (27), Eq. (28) and Eq. (29) the analytical solution developed for the GSS model can be expressed as a function of the system parameters, x and $\bar{\theta}$ as,

$$\{Z(x)\} = \begin{Bmatrix} g_1(x) \\ g_2(x) \\ g_3(x) \\ g_4(x) \\ g_5(x) \\ g_6(x) \end{Bmatrix} \bar{\theta} \tag{30}$$

From Eq. (10), the transfer function for the rigid hub rotation, $\bar{\theta}$, can be expressed as,

$$\mu^2 \left[J + m(r+L)g_3(L) + I_{\text{tip}}g_4(L) + \rho\left((r+x)g_2(x) - g_1(x)\right) \right] \bar{\theta} = \bar{u}$$

$$\bar{\theta} = \frac{\bar{u}}{\mu^2 \left[J + m(r+L)g_3(L) + I_{\text{tip}}g_4(L) + \rho\left((r+x)g_2(x) - g_1(x)\right) \right]} \tag{31}$$

From the GSS model presented in Eq. (12) and Eq. (30), $\bar{y}$ can be expressed as,

$$\bar{y} = g_3(x)\bar{\theta} \tag{32}$$

Substituting Eq. (31) into Eq. (32) yields the flexible appendage transfer function with the torque $\bar{u}$ as input,

$$\bar{y} = \frac{g_3(x)}{\mu^2 \left[J + m(r+L)g_3(L) + I_{\text{tip}}g_4(L) + \rho\left((r+x)g_2(x) - g_1(x)\right) \right]} \bar{u} \tag{33}$$

IV.B. The assumed modes approach

The assumed modes solution has been a very reliable technique in addressing structural systems,.[21] Following the approach presented in[4] the assumed modes approach is used as the numerical counterpart of the analytical results presented in the previous section. In this approach the spatial and the time dependent components of the beam response in Eq. (6) are decoupled by assuming the seperation of variables series solution,

$$y(x,t) = \sum_{i=1}^{N} q_i(t)\phi_i(x) \tag{34}$$

The admissible function $\phi_i(x)$ describing the i-th spatial mode of the flexible appendage is defined as,

$$\phi_i(x) = 1 - \frac{\cos(i\pi x)}{L} + \frac{1}{2}(-1)^{i+1}\left(\frac{i\pi x}{L}\right)^2 \tag{35}$$

$$\text{where, } 0 \le x \le L$$

Using Eq. (34) and Eq. (35) with Eq. (3) and Eq. (4) and following the Lagrangian approach,

$$\frac{d}{dt}\left(\frac{\partial T}{\partial \mathbf{x}}\right) - \frac{\partial T}{\partial \mathbf{x}} + \frac{\partial V}{\partial \mathbf{x}} = \mathbf{F} \tag{36}$$

the system of equations of motion is represented in the matrix form,

$$\begin{bmatrix} J & M_{\theta q}^{\mathrm{T}} \\ M_{\theta q} & M_{qq} \end{bmatrix} \ddot{\mathbf{x}} + \begin{bmatrix} 0 & 0 \\ 0 & K_{qq} \end{bmatrix} \mathbf{x} = \begin{Bmatrix} u \\ 0 \end{Bmatrix} \tag{37}$$

where the elements of the mass and the stiffness matrices are defined as,

$$J = I_{\text{hub}} + m(r+L)^2 + I_{\text{tip}} + \int_0^L \rho(r+x)^2 \, \mathrm{d}x$$

$$[M_{\theta q}]_i = \rho \int_0^L (r+x)\phi_i(x) \, \mathrm{d}x + m(r+L)\phi_i(L) + I_{\text{tip}}\phi_i'(L) \tag{38}$$

$$[K_{qq}]_{ij} = \int_0^L \phi_i''(x)\phi_j''(x) \, \mathrm{d}x$$

The natural frequencies of the flexible mode can then be computed from solving the eigenvalue problem for Eq. (37). Table 2 shows the first six flexible modes as calculated from solving the eigenvalue problem using 20 modes to construct the problem,

Table 2. Natural frequencies of the flexible appendage

Mode Number	Natural Frequency ω (rad/sec)
1	5.531
2	51.7566
3	156.6555
4	306.0268
5	497.9744
6	751.0886

IV.C. GSS transfer function vs. Assumed modes frequency response

In this section a numerical comparison is conducted for the frequency response of the flexible appendage calculated from the transfer function presented in Eq. (33) and the assumed modes solution presented in table 2. Several ranges of natural frequencies, ω, are swept and the frequency responses for both the GSS transfer function and the assumed modes are plotted. Figure 4shows the comparison for the first mode, figure 5 highlights the second mode and figure 6 shows the range from the third to the sixth modes.
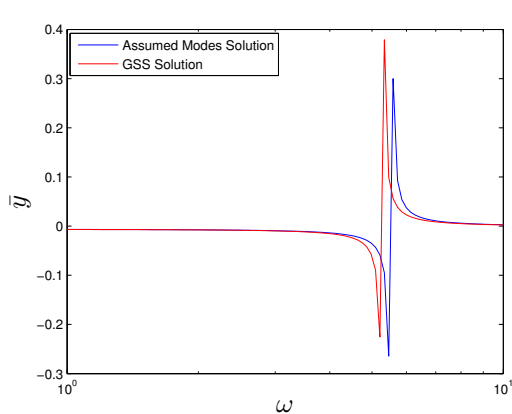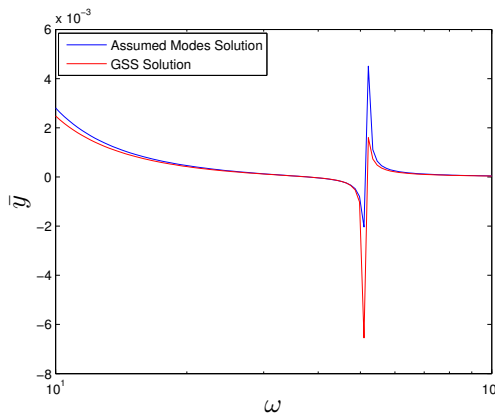

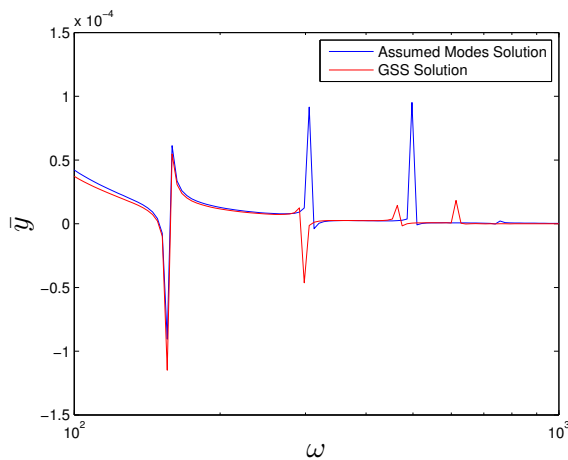**Figure 4. First flexible mode**

Figure 5. Second flexible mode

Figure 6. Third to sixth flexible modes

American Institute of Aeronautics and Astronautics

The closed form frequency response presented agrees with and validates the numerical approximation of the assumed modes. Truncation resulting from the assumed modes approximation can be highlighted when compared to the accurate closed form results provided by the GSS transfer function. As expected the series solution is seen to converge from above. In this case the second mode is accurately captured by both methods. The first mode, however, is not captured well. For the shown range of frequencies the GSS solution proved to be more accurate and free of truncation errors associated with approximated solution. These results can be compared to more accurate numerical approximations utilizing finite elements or higher order assumed modes to verify the achieved accuracy. Furthermore, by knowing the exact frequency response of the system the door is open for more accurate controls schemes.

V.   Conclusion

The hybrid rigid-flex model presented here is a widely used approximation for a rotating flexible spacecraft. The spacecraft is modeled as a three body system comprising a rigid rotating hub, a flexible appendage and a point mass at the tip. The appendage is assumed to follow the Euler-Bernoulli's beam assumptions. Lagrange's equation combined with Hamilton's extended principle are used to derive the system equations of motion and their associated boundary conditions. A key step is implemented by utilizing integration by parts in the rigid mode equation to take out the explicit spatial dependency of the integral terms resulting from the coupling between the rigid and the flexible modes. Laplace transform is then applied to the equations of motion to formulate a frequency domain generalized state space system of equations. In order to solve the linear system of equations the beam sub-problem is first addressed using the eigen decomposition method to solve the matrix exponential problem. Results from the beam sub-problem are then used to solve for the full system of equations. The solution is then represented as the real part of a much simpler complex function that simplified the full solution to a single trigonometric function and its second and third order derivatives. The boundary conditions are applied to solve for the state variables in terms of the known system parameters. First, z_5 and z_6 are solved in term of $z_3(L)$ and $z_4(L)$, the third and fourth state variables evaluated at the beam tip. Then, $z_3(L)$ and $z_4(L)$ are solved for in terms of the system parameters and back substituted into z_5 and z_6 to complete the full closed form solution.

The closed form solution is verified versus numerical integration of the GSS system of equations and the results agree to the extent of the machine precision. To further investigate the frequency response of the system the closed form solution is used to generate input/output transfer function for both the rigid and the flexible modes of the system. The frequency response of the transfer function is then compared to the eigenvalues analysis resulting from the assumed modes approach. The presented numerical example clearly highlights the truncation of the series in the assumed modes solution and the higher accuracy of the closed form solution. The convergence also appears to occur from above which verifies the validity of the closed form solution.

The resulting frequency domain analysis is a step to accurately calculate the natural frequencies of such complicated hybrid systems. The existence of such accurate solution can extend to controls and optimization applications. Also in the field of robotics the same model can be utilized for the optimization and control of a flexible robotic appendage with and without a payload. Such applications can benefit tremendously from the existence of the presented exact solution to better understand and control hybrid systems.

References

[1] Santini, P. and Gasbarri, P., "Dynamics of multibody systems in space environment; Lagrangian vs. Eulerian approach," *Acta Astronautica*, Vol. 54, No. 1, 2004, pp. 1–24.

[2] Meirovitch, L. and Quinn, R., "Equations of motion for maneuvering flexible spacecraft," *Journal of Guidance, Control, and Dynamics*, Vol. 10, No. 5, 1987.

[3] Meirovitch, L. and Stemple, T., "Hybrid equations of motion for flexible multibody systems using quasicoordinates," *Journal of Guidance, Control, and Dynamics*, Vol. 18, No. 4, 1995.

[4] Junkins, J. L. and Kim, Y., *Introduction to dynamics and control of flexible structures*, Elsevier Science Publishers, 1986.

[5] Lee, S. and Junkins, J. L., "Explicit generalizations of Lagrange's equations for hybrid coordinate dynamical systems," *Journal of Guidance, Control, and Dynamics*, Vol. 15, No. 6, 1992.

[6] HALE, A. L., Lisowski, R. J., and DAHL, W. E., "Optimal simultaneous structural and control design of maneuvering flexible spacecraft," *Journal of Guidance, Control, and Dynamics*, Vol. 8, No. 1, 1985.

[7] Junkins, J. and Turner, J., *Optimal spacecraft rotational maneuvers*, Elsevier, 1986.

[8] Turner, J. and Junkins, J., "Optimal large-angle single-axis rotational maneuvers of flexible spacecraft," *Journal of Guidance, Control, and Dynamics*, Vol. 3, No. 6, 1980.

[9] Turner, J. and Chun, H., "Optimal distributed control of a flexible spacecraft during a large-angle maneuver," *Journal of Guidance, Control, and Dynamics*, 1984.

[10] Maganti, G. B. and Singh, S. N., "Simplified adaptive control of an orbiting flexible spacecraft," *Acta Astronautica*, Vol. 61, No. 7, 2007, pp. 575 – 589.

[11] Junkins, J., Rahman, Z., and Bang, H., "Near-minimum-time control of distributed parameter systems-Analytical and experimental results," *Journal of Guidance, Control, and Dynamics*, Vol. 14, No. 2, 1991.

[12] Breakwell, J., "Optimal feedback slewing of flexible spacecraft," *Journal of Guidance, Control, and Dynamics*, Vol. 4, No. 5, 1981.

[13] Ben-Asher, J., Burns, J., and Cliff, E., "Time-optimal slewing of flexible spacecraft," *Journal of guidance, control, and dynamics*, Vol. 15, No. 2, 1992.

[14] Singh, G., Kabamba, P., and McClamroch, N., "Planar, time-optimal, rest-to-rest slewing maneuvers of flexible spacecraft," *Journal of Guidance, Control, and Dynamics*, Vol. 12, No. 1, 1989.

[15] Wie, B., Sinha, R., and Liu, Q., "Robust time-optimal control of uncertain structural dynamic systems," *Journal of Guidance, Control, and Dynamics*, Vol. 16, No. 5, 1993.

[16] Boškovic, J., Li, S., and Mehra, R., "Robust adaptive variable structure control of spacecraft under control input saturation," *Journal of Guidance, Control, and Dynamics*, Vol. 24, No. 1, 2001.

[17] Dwivedy, S. and Eberhard, P., "Dynamic analysis of flexible manipulators, a literature review," *Mechanism and Machine Theory*, Vol. 41, No. 7, 2006, pp. 749–777.

[18] Turner, J. D. and Elgohary, T. A., "Generalized Frequency Domain State-Space Models for Analyzing Flexible Rotating Spacecraft," *Advances in Astronautical Sciences*, Vol. 139, 2011.

[19] Meirovitch, L., *Methods of analytical dynamics*, Dover Publications, 2010.

[20] Chen, C. T., *Linear System Theory and Design*, Oxford University Press, 1998.

[21] Hurty, W., "Dynamic analysis of structural systems using component modes," *AIAA journal*, Vol. 3, No. 4, 1965.